Resonance in asymmetric warped geometry

Gregory Gabadadze, Luca Grisa and Yanwen Shang

Center for Cosmology and Particle Physics
Department of Physics, New York University, New York, NY, 10003, U.S.A.
E-mail: `gabadadze@physics.nyu.edu`, `luca.grisa@nyu.edu`,
`yanwen.shang@physics.nyu.edu`

ABSTRACT: We study the spectrum of an asymmetric warped braneworld model with different AdS curvatures on either side of the brane. In addition to the RS-like modes we find a resonance state. Its mass is proportional to the geometric mean of the two AdS curvature scales, while the difference between them determines the strength of the resonance peak. There is a complementarity between the RS zero-mode and the resonance: making the asymmetry stronger weakens the zero-mode but strengthens the resonance, and vice versa. We calculate numerically the braneworld gravitational potential and discuss the holographic correspondence for the asymmetric model.

JHEP08(2006)033

Contents

1. Introduction

In the RS2 model [1] a significant role is played by the $\mathbb{Z}_2$ orbifold: The wavefunctions of gravitational perturbation that are antisymmetric across the brane are projected out. On the other hand, one could consider more general geometries in which the AdS curvatures on either side of the brane are different. Such branes can emerge as consistent solitonic solutions in 5D $\mathcal{N} = 1$ supergravities [2]. These domain walls interpolate between the AdS vacua with different cosmological constants, and are stable as they saturate the BPS bound. Given the special properties of the RS spectrum, and its relevance for holography, it appears interesting to study similar issues in the braneworld with the asymmetric bulk geometry. Some of the properties of the asymmetric models were discussed previously, see, e.g. [3–5]. In particular, the present work was motivated by ref. [4], which argued that the asymmetric model could provide UV completion to brane induced gravity [6]. If true, such a model could be used to look at the strong coupling dynamics in [6], from a different perspective. Below, we will give comprehensive studies of the spectrum and emphasize the similarities and differences of our results with the earlier ones.

At energies that exceed the AdS curvature scales (but are still below the quantum gravity scale), both the RS2 and asymmetric model are expected to have similar behavior. On the other hand, at energies comparable to, or somewhat below of the AdS curvature scales, the asymmetric model should behave differently from RS2. Let us denote by $k_\pm^2$ the two AdS curvatures, assuming for definiteness $k_- < k_+$. At energies below k_- one can "integrate out" a slice of AdS_+ space. In the holographic description this corresponds to integrating out modes in the energy/momentum interval $k_- < E < k_+$. The result is the RS2 model with AdS curvature k_- on both sides, in which, however, the orbifold projection

is not imposed (i.e., the antisymmetric perturbations are kept). Moreover, in the low energy theory, while integrating out the slice of AdS, the brane-induced Einstein-Hilbert (EH) term will appear. The coefficient in front of this term is going to be proportional to $(k_+^2 - k_-^2)/k_+^3$. Hence, at energies below k_-, the original asymmetric model reduces to the RS2 model without the orbifold projection and with the brane-induced EH term, similar to [6].

The properties of this hybrid low-energy model are well understood [7]. At energies above the scale $m_* \sim k_+^3/(k_+^2 - k_-^2)$ gravity is similar to that of the DGP model [6]. However, in the present construction this regime can not be reached, since the effective description in terms of the induced EH term is valid only at energies below k_-, which is always smaller than m_*. Therefore, the DGP phase, emphasized in ref. [4], does not seem to be attainable in the asymmetric braneworld scenario.[1] Nevertheless, as we will describe below, the asymmetric models exhibits a number of interesting properties. The RS zero-mode is still present, as long as both AdS curvatures are nonzero. Moreover, because of the absence of the orbifold projection, both symmetric and antisymmetric modes survive. Conventionally, these modes can be grouped into two sets. One set has properties similar to the RS spectrum [1]. The net result of the second set is a resonance state[2] with the mass $\sim \sqrt{k_- k_+}$, and width $\sim k_+$. The strength of the resonance peak is proportional to the difference of the the two AdS curvatures. It vanishes in the limit when the two curvatures are equal, and the corresponding set of states turns into the antisymmetric modes that are projected out from the RS model by the $\mathbb{Z}_2$ orbifold.

The paper is organized as follows. In section 2, we set the action for the asymmetric model and discuss its general features. In section 3 we derive the complete spectrum of linearized perturbations and discuss some of its properties and implications. In section 4 we calculate the gravitational potential as seen by a braneworld observer in the asymmetric model and compare it with the potential of the RS2 model. The RS model has been extensively studied from the point of view of its holographic dual. It seems reasonable to expect that the asymmetric model also has a holographic description. We discuss these issues in section 5. Conclusions are given in section 6.

2. General formalism in the asymmetric setup

The action of the braneworld with asymmetric warped geometry is given by

$$S = \int \mathrm{d}^4 x \int_{y>0} \mathrm{d}y \sqrt{-g} M_*^3 \{2R + 24k_+^2\} + \int \mathrm{d}^4 x \int_{y<0} \mathrm{d}y \sqrt{-g} M_*^3 \{2R + 24k_-^2\} +$$
$$+ \int_{\mathrm{brane}} \mathrm{d}^4 x \sqrt{-g^*} \{\tau + \mathcal{L}_{\mathrm{SM}}\}. \tag{2.1}$$

---

[1]It was claimed in [3] that the DGP phase can be reached if different 5D Planck scales are assumed on two different sides of the brane. However, one could perform asymmetric conformal transformations in the bulk to equate the Planck scales on both sides, at the expense of changing the nature of the junction condition across the brane. In the present work we will not consider such a possibility since the brane we keep in mind is a solitonic domain wall solution of the type of ref. [2], that arises in a theory with a fixed 5D Planck scale. In principle, the asymmetry in the 5D Planck scales could potentially be generated by an asymmetric profile of a dilaton-type field.

[2]A resonance in braneworlds was first discussed in refs. [8], in a different setup.

The brane is located at $y = 0$ where all the localized matter/gauge (called "the Standard Model") fields live. If the brane tension τ is fine-tuned to be $12M_*^3(k_+ + k_-)$, we have the following solution for the metric in the bulk:

$$\begin{aligned}
\mathrm{d}s^2 &= e^{-2k_+|y|}\mathrm{d}x^\mu \mathrm{d}x_\mu - \mathrm{d}y^2, \quad \text{for } y > 0, \quad \text{and} \\
\mathrm{d}s^2 &= e^{-2k_-|y|}\mathrm{d}x^\mu \mathrm{d}x_\mu - \mathrm{d}y^2, \quad \text{for } y < 0.
\end{aligned} \tag{2.2}$$

Indices μ, ν run over directions along the brane. One could think of this geometry as being two half-AdS spaces glued together across the brane at $y = 0$. k_+^2 and k_-^2 are the AdS curvatures on two sides of the brane. In general they are different and we define the ratio

$$\eta \equiv \frac{k_-}{k_+}, \tag{2.3}$$

as a measure of the "asymmetry" of the model.

There are questions concerning the stability of the setup. First, as we will show below, the small fluctuations in the model contain no tachyon or ghost modes. Second, because of the asymmetry of the bulk cosmological constants, one may worry about the stability of the system with respect to the motion of the brane as a whole. However, when such a motion occurs, the gravitational background readjusts itself so that there is no net energy gain/loss on either side of the brane. Hence, there is no reason for such an instability. This is of course consistent with the brane being a bosonic part of a supersymmetric BPS object [2]. The instability that could in general occur in the purely bosonic asymmetric case, is due to nonperturbative tunneling from one vacuum to the other via bubble nucleation process. However, this processes can be made exponentially small by appropriate choice of the parameters, and will be ignored below.

Following [1] we consider small gravitational perturbations $G_{\mu\nu} = e^{-2k_\pm|y|}(\eta_{\mu\nu} + h_{\pm\,\mu\nu}(x,y))$ in the gauge $\partial^\mu h_{\pm\,\mu\nu} = h_{\pm\,\mu}{}^\mu = 0$. We can choose this gauge and keep the brane straight at $y = 0$ in a source-free approximation. Performing the coordinate transformation

$$z \equiv sgn(y)\left(e^{k_\pm|y|} - 1\right)/k_\pm,$$

and field redefinition $h_{\pm\,\mu\nu} \equiv \psi_{\pm\,\mu\nu}^{(m)} e^{-|k_\pm|y/2}e^{ipx}$, where $m^2 \equiv p^2$, we find the "Schrödinger" equation for $\psi^{(m)}$. Ignoring the tensorial structure it reads

$$[-\frac{1}{2}\partial_z^2 + V_\pm(z)]\psi_\pm^{(m)}(z) = m^2\psi_\pm^{(m)}(z), \tag{2.4}$$

where the potential is given by

$$V_\pm(z) = \frac{15k_\pm^2}{8(k_\pm|z| + 1)^2} - \frac{3}{4}(k_+ + k_-)\delta(z). \tag{2.5}$$

This potential is sketched in figure 1 with the δ-function regularized. It differs from that for the RS model as the heights of the two barriers on different sides of the brane are not equal.

We can identify four regimes for the potential: (1). Above both barriers, the gravity should behave as a 5-D theory; (2). at energies between the two peaks, one would expect
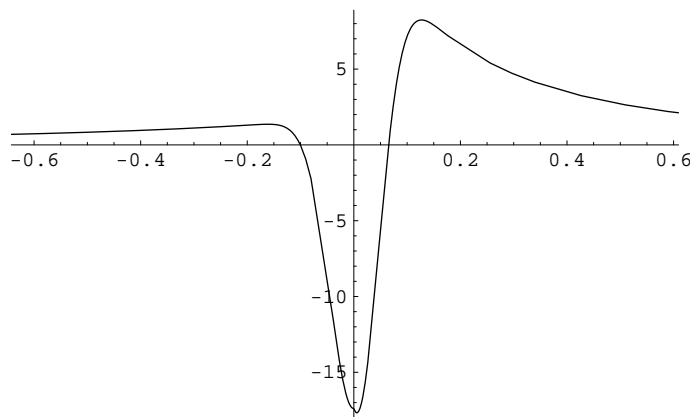
Figure 1: Potential $V(z)$ where the δ-function is regularized.

novelties since this regime is absent in RS2; gravitons of such energies can pass the barrier through tunneling on one side, but they are allowed to freely propagate on the other side as their energy is above the peak; (3). Below both barriers we are in what could be called the RS-phase, where we expect the model to exhibit properties similar to RS. Furthermore, the zero-mode, if exists, is localized on the brane and gives rise to effective 4-D interactions.

General solution of this equation can be found as

$$\psi_{\pm}^{(m)}(z) = (|z| + 1/k_{\pm})^{1/2} \left[A_{\pm} Y_2(m(|z| + 1/k_{\pm})) + B_{\pm} J_2(m(|z| + 1/k_{\pm})) \right]. \tag{2.6}$$

Here and below Y_2 and J_2 are Bessel functions and $A_{\pm}$ and $B_{\pm}$ are constant coefficients to be determined by boundary conditions. The junction conditions across the brane are

$$\psi_{+}^{(m)}(0) = \psi_{-}^{(m)}(0), \quad \text{and} \quad \psi_{+}^{(m)}(0)' - \psi_{-}^{(m)}(0)' + \frac{3}{2}(k_+ + k_-)\psi^{(m)}(0) = 0, \tag{2.7}$$

where the derivative is with respect to z.

We normalize the wave functions in the following way. While $z \to \pm\infty$ all wave-functions $\psi_{\pm}^{(m)}(z)$ asymptote to plain waves. It can be checked that this is equivalent to the usual orthonormal condition in the limit $L \to +\infty$, where L is the distance in the z-coordinate between the brane-world and a fictitious regulator brane. Since for $z \to \pm\infty$,

$$\sqrt{z}Y_2(mz) \sim \sqrt{\frac{2}{\pi m}} \sin\left(mz - \frac{5}{4}\pi\right), \quad \sqrt{z}J_2(mz) \sim \sqrt{\frac{2}{\pi m}} \cos\left(mz - \frac{5}{4}\pi\right), \tag{2.8}$$

it is natural to parametrize the normalization coefficients as:

$$\psi_{\pm}^{(m)}(z) = \epsilon_{\pm} \sqrt{\frac{\pi m(|z| + 1/k_{\pm})}{2(1 + \alpha_{\pm}^2)}} \left[\alpha_{\pm} Y_2(m(|z| + 1/k_{\pm})) + J_2(m(|z| + 1/k_{\pm})) \right], \tag{2.9}$$

with $\alpha_{\pm}$ to be determined by the junction conditions (2.7). Using the properties of the Bessel's functions, they are found to be

$$\frac{\epsilon_+}{\sqrt{k_+(1 + \alpha_+^2)}}[\alpha_+ Y_{2+} + J_{2+}] = \frac{\epsilon_-}{\sqrt{k_-(1 + \alpha_-^2)}}[\alpha_- Y_{2-} + J_{2-}], \tag{2.10}$$

$$\frac{\epsilon_+}{\sqrt{k_+(1+\alpha_+^2)}}[\alpha_+ Y_{1+} + J_{1+}] = -\frac{\epsilon_-}{\sqrt{k_-(1+\alpha_-^2)}}[\alpha_- Y_{1-} + J_{1-}]. \tag{2.11}$$

Here $Y_{1,2\pm} \equiv Y_{1,2}(m/k_\pm)$ and $J_{1,2\pm} \equiv J_{1,2}(m/k_\pm)$.

We have introduced the sign factors $\epsilon_\pm$ in the parametrizations above. They are functions of $m/k_\pm$ and take the values of ± 1 only.[3]

In the limiting case when one of the k's is 0, the wave-functions on the flat side turn into plane waves. Both equations (2.10) and (2.11) are simplified in this case. Assuming that the "$-$"-side is flat, the wave-functions are simply given by $\psi^{(m)}(z) = \sin(mz + \beta)$, with a phase shift angle β to be determined by the junction conditions. The latter, derived directly from (2.7), are

$$\sqrt{\frac{\pi m}{2k(1+\alpha^2)}}[\alpha Y_2(m/k) + J_2(m/k)] = \sin\beta, \tag{2.12}$$

$$\sqrt{\frac{\pi m}{2k(1+\alpha^2)}}[\alpha Y_1(m/k) + J_1(m/k)] = -\cos\beta. \tag{2.13}$$

We have omitted all the $+$ signs for the quantities on the l.h.s. of the two equations above. It is no longer necessary to include the sign factor ϵ_+ since it can always be absorbed into the redefinition of β.

3. Spectrum and its properties

In the following section we will discuss in details the solutions to the boundary conditions described above. First we verify whether the zero-mode of the RS model still exists in the asymmetric scenario. As we will see this indeed is the case, however, the zero-mode becomes weaker as one of the AdS curvatures decreases and disappears completely from the spectrum if the bulk space-time on one side is flat. Regarding the massive KK modes, we will find that alongside the RS-like modes, there exists a new solution in the asymmetric scenario which behaves as a resonance.

3.1 Zero-mode wave function

In the RS2 model, the zero-mode is localized on the brane and there it gives rise to the usual 4-D gravity at low energy. In the asymmetric case, the "Schrödinger" equation for the zero-mode reads

$$\left[-\frac{1}{2}\partial_z^2 + V(z)\right]\psi_0(z) = 0, \tag{3.1}$$

where $V(z)$ is the potential defined in the previous section (2.5). For generic k_+ and k_-, the normalized solution to this equation can be found as

$$\psi_0(z) = \sqrt{\frac{2k_- k_+}{k_- + k_+}}\left[\frac{\theta(-z)}{(k_-|z|+1)^{3/2}} + \frac{\theta(z)}{(k_+|z|+1)^{3/2}}\right], \tag{3.2}$$

which is plotted in figure 2. Here $\theta(x)$ is the step function. This zero-mode is localized.

---

[3]In solving the junction conditions one has to take the square of the ratio of the two equations. Doing so the sign becomes ill-defined. To recover it, we must choose the sign-factors $\epsilon_\pm$ accordingly.
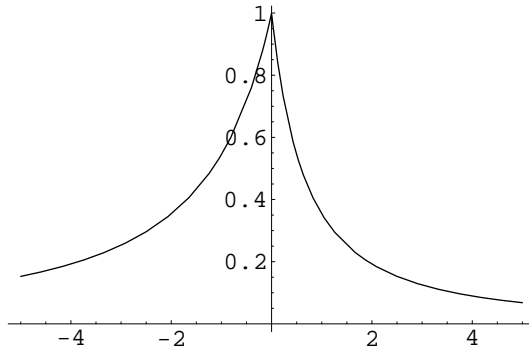
Figure 2: Behavior of the zero-mode wave-function with $k_- = .2$ and $k_+ = 1$.

The localization width is proportional to $1/k_-$ on the left side and to $1/k_+$ on the right. The prefactor of the wave-function is determined by fixing the norm of $\psi(z)$ to be 1. This sets the relation between the bulk Planck mass M_* and 4-D Planck mass measured on the brane as

$$M_{\rm pl}^2 = M_*^3 \left(\frac{1}{k_+} + \frac{1}{k_-} \right). \tag{3.3}$$

Notice that as one of the two AdS curvatures decreases, this zero-mode gradually delocalizes in the extra dimension while the effective 4-D Newton coupling tends to zero. Eventually, if the bulk space on one side of the brane is flat, the wave-function of the zero-mode becomes non-normalizable. Indeed as $k_- \to 0$ the overall multiplicative factor $[2k_+k_-/(k_+ + k_-)]^{1/2}$ goes to zero. Therefore in this limit the strength of the zero-mode vanishes on the brane. Equivalently the effective 4-D Planck mass becomes infinite, and Newton's constant tends to zero.

3.2 Spectrum for $k_- = 0$ and $k_+ \neq 0$

We now turn to the massive modes. As a warm-up, we first discuss the spectrum in a simpler case where one of the curvatures vanishes so that the bulk space-time on one side of the brane is flat. The boundary conditions are given by equations (2.12) and (2.13). In the limit $m/k \ll 1$, their solutions can be explicitly found. In the leading order of the m/k expansion

$$Y_2(m/k) \sim -\frac{4k^2}{\pi m^2}, \quad Y_1(m/k) \sim -\frac{2k}{\pi m} \qquad \text{and}$$
$$J_2(m/k) \sim \frac{m^2}{8k^2}, \quad J_1(m/k) \sim \frac{m}{2k}. \tag{3.4}$$

It is reasonable to expect that, in the limit $m/k \ll 1$, the Y-terms in both equations dominate; this has to be verified on the solution by checking how the constant α defined in (2.9) scales with m/k.

With these approximations we find

$$-\tan\beta = \frac{Y_2(m/k)}{Y_1(m/k)} = \frac{2k}{m}, \tag{3.5}$$

and, therefore, the strength of the KK modes on the brane is given by

$$\psi^{(m)}(0)^2 = \sin^2 \beta = \frac{1}{1 + m^2/4k^2}. \qquad (3.6)$$

It is interesting to point out that this solution has a similar form as that of the DGP model [6, 10], with the crossover distance $r_c = 1/(2k)$. This was first noticed by the authors of [4]. We will discuss the physical significance of this similarity in subsection 3.4.

First we check that our approximation is consistent. Notice that in this approximation

$$\alpha \sim \sqrt{\frac{m}{k}} \frac{m}{k}. \qquad (3.7)$$

One can easily verify that in both equation (2.12) and (2.13), Y-terms do dominate as expected.

Exact solutions to (2.12) and (2.13) can be found by solving the quadratic equations. The strengths of the KK modes on the brane are given as follows:

$$\Delta = \frac{2k}{\pi m}(Y_1^2 + Y_2^2 + J_1^2 + J_2^2) - \frac{4k^2}{\pi^2 m^2} - (Y_1 J_2 - Y_2 J_1)^2, \qquad (3.8)$$

$$\alpha_{1,2} = \frac{-(Y_1 J_1 + Y_2 J_2) \pm \sqrt{\Delta}}{Y_1^2 + Y_2^2 - 2k/(\pi m)}, \qquad (3.9)$$

$$\psi_{1,2}^{(m)}(0)^2 = \frac{\pi m}{2k(1 + \alpha_{1,2}^2)}[\alpha_{1,2} Y_2 + J_2]^2. \qquad (3.10)$$

We find that there exist two different solutions. On figure 3 we plot both $\psi_{1,2}^{(m)}(0)^2$ as functions of m/k. Just for comparison we also plot the DGP spectrum with $r_c = 1/(2k)$.

As we see there exists a part of the spectrum that is almost constant. This is of course expected. When we have a flat space on one side of the brane, KK gravitons of arbitrary energy can easily probe into the bulk.[4] However, in addition to the "flat" spectrum there exists a new solution which has a resonance type behavior. The peak of this resonance is located at $m = 0$ and its width is of the order of the curvature on the AdS side.

An immediate question following these observations arises. Does this new resonance state persist for arbitrary values of $k_+ \neq k_-$? This is the issue that we will address in the next subsection.

3.3 General spectrum for $k_+ k_- \neq 0$

When both $k_\pm \neq 0$ and are not equal to each other, one must solve equation (2.10) and (2.11) exactly. We give below the square of the strengths of the two solutions on the brane at $z = 0$. Defining

$$\eta \equiv \frac{k_-}{k_+}, \qquad (3.11)$$

---

[4]The "flat" spectrum is not exactly flat, but around masses of the order of the AdS curvature it departs from being constant showing a tiny structure as shown in figure 4. This is expected since at that mass scale the graviton mode can tunnel into the curved side of the brane.
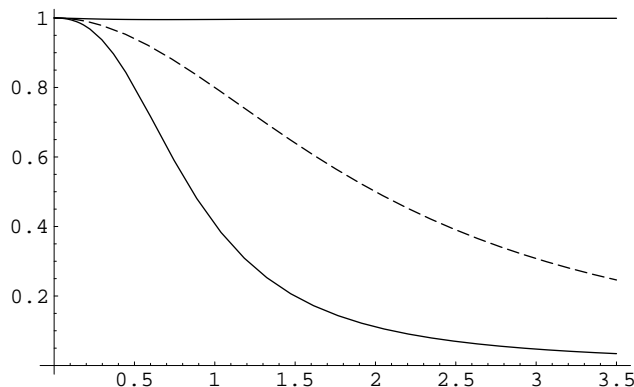
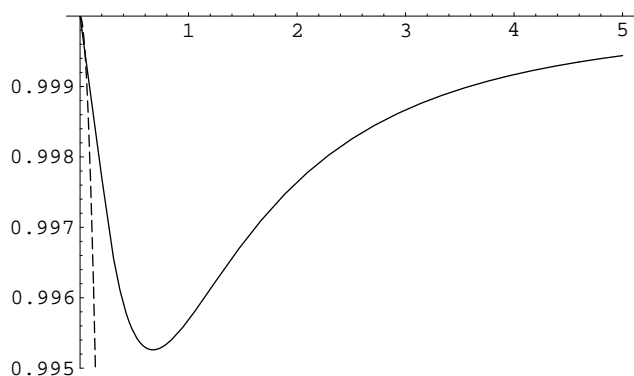**Figure 3:** $\psi^{(m)}(0)^2 \sim m/k$. Dashed curve is for the DGP model.

Figure 4: $\psi^{(m)}(0)^2 \sim m/k$. Small structure of the "flat" solution plotted alone. Dashed curve is for the DGP model.

$$A = \eta\left[(J_{2-}Y_{1+} + J_{1-}Y_{2+})(J_{1+}J_{2-} + J_{2+}J_{1-}) + \\ + (Y_{1+}Y_{2-} + Y_{1-}Y_{2+})(J_{1+}Y_{2-} + J_{2+}Y_{1-})\right], \tag{3.12}$$

$$B = \frac{2k_-}{\pi m} \cdot \sqrt{\begin{array}{l} \eta[(J_{2-}Y_{1+} + J_{1-}Y_{2+})^2 + (J_{1+}J_{2-} + J_{2+}J_{1-})^2 + \\ + (Y_{1+}Y_{2-} + Y_{1-}Y_{2+})^2 + (J_{1+}Y_{2-} + J_{2+}Y_{1-})^2] + \\ -\eta^2[(J_{1+}Y_{2+} - J_{2+}Y_{1+})^2 + 4k_+^2/(\pi m)^2] \end{array}}, \tag{3.13}$$

$$D = -\eta[(Y_{1+}Y_{2-} + Y_{1-}Y_{2+})^2 + (J_{2-}Y_{1+} + J_{1-}Y_{2+})^2] + \left(\frac{2k_-}{\pi m}\right)^2, \tag{3.14}$$

on the brane, the two solutions are given by

$$\psi_1^{(m)}(0)^2 = \frac{\pi m}{k_+} \frac{[J_{2+}D + Y_{2+}(A - B)]^2}{2[D^2 + (A - B)^2]}, \tag{3.15}$$

$$\psi_2^{(m)}(0)^2 = \frac{\pi m}{k_+} \frac{[J_{2+}D + Y_{2+}(A + B)]^2}{2[D^2 + (A + B)^2]}. \tag{3.16}$$
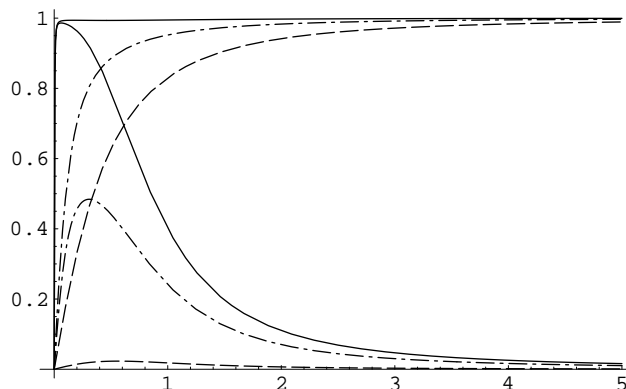
Figure 5: Two solutions $\psi_{1,2}^{(m)}(0)^2$ (Y-axis) $\sim m/k_+$, with different values of $\eta = 0.005$ (solid line), 0.2 (dashed-dot line) and 0.75 (dashed line).

The solutions with different values of η are plotted on figure 5. There are always two distinct solutions. One of them resembles the RS KK spectrum, and it will be referred to as the RS-like spectrum. The other one has a resonance type behavior and will be referred to as the resonance mode.

Some comments on the qualitative properties of the two spectra are in order. First of all, when $\eta \to 1$ the strength of the resonance mode on the brane decreases and tends to zero. This confirms the argument we have made in the introduction: in the RS limit, the new modes we are considering becomes anti-symmetric wave-functions and automatically vanishes on the brane. In the original RS model they are modded out by orbifolding the extra dimension. Only when we split k_+ from k_-, we no longer have any symmetry reason to discriminate between the two solutions. Neither of them is symmetric or anti-symmetric any more and we must retain them both.

On the other hand, when $\eta \to 0$, or $+\infty$, i.e., when one of the two sides is flat, we recover the results found in the previous subsection.

It is a right place here to emphasize that the zero-mode strength is given by

$$|\psi^0(0)| = \sqrt{\frac{2k_- k_+}{k_- + k_+}}. \tag{3.17}$$

When $\eta \to 0$ it vanishes while the resonance reaches its maximal strength. On the other hand, the zero-mode has its maximal strength in the RS limit when the resonance decouples. We see that there is a complementarity between the resonance and zero-mode: when one disappears the other is present, and *vice versa*. When k_- differs from k_+, the amplitude of the zero-mode weakens in favor of the resonance.

Finally we point out that in the small m/k_+ region, when η is sufficiently different from 1, the once smooth RS-like spectrum starts developing a little distortion. That is how, when η changes, the spectrum deforms and links between the smooth RS-spectrum ($\eta = 1$) and the almost flat one ($\eta = 0$), discussed in the previous subsection. Figure 6 demonstrates such a behavior.
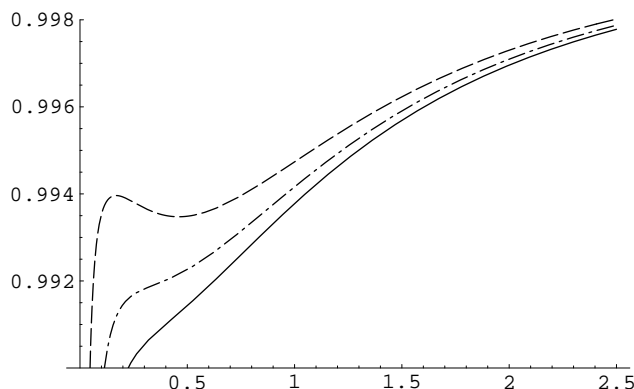
Figure 6: $\psi_1^{(m)}(0)^2$ (Y-axis) $\sim m/k_+$, with $\eta = 0.01$ (solid line), 0.008 (dashed-dot line) and 0.005 (dashed line) respectively.

It can be checked that when $m \ll \sqrt{k_+ k_-}$, both our solutions are approximately linear in m, in particular

$$|\psi_2^{(m)}|^2 \sim \frac{\pi(1 - \eta^{3/2})^2}{\eta(1+\eta)^2} m. \tag{3.18}$$

On the other hand, in the limit $m \to \infty$, the RS mode approaches 1 and the new mode tends to 0 as $1/m^2$.

3.4 On mixing and on resonance mass

First we turn to an important question: Are the two distinct KK sectors orthogonal to each other? If they were not, in the effective action on the 4-D brane, a mixing term of the two graviton modes would appear with a mixing coefficient f_m.

In the RS limit the two solutions are symmetric and anti-symmetric wave-function respectively and are orthogonal.

To calculate the mixing $f_m = \int \mathrm{d}z \psi_1^{(m)}(z) \psi_2^{(m)}(z) / \int \mathrm{d}z$, we follow the normalization procedure described in [1]. Introduce the regulator branes at $z_{c\pm}$ on both sides of the brane and correspondingly impose the new boundary condition there:

$$\partial_z \psi_{\pm}^{(m)}(z_{c\pm}) = -\frac{3k_{\pm}}{2(k_{\pm} z_{c\pm} + 1)} \psi_{\pm}^{(m)}(z_{c\pm}). \tag{3.19}$$

The zero-mode satisfies this condition and remains unchanged. When the regulator brane is at a finite distance from the brane where matter is localized, these conditions will quantize the KK masses in units of $1/z_{c\pm}$. For simplicity we fix $z_{c+} = z_{c-} = z_c$ so that the discretized mass spectrum is equally distributed. In general, one could set both $z_{c\pm}$ arbitrarily, but the result is a more complicated discretization of the mass spectrum of KK gravitons since boundary conditions on both regulator branes must be satisfied simultaneously. This, in principle, must give the same physical results when both regulator branes are taken to infinity but is mathematically more difficult to deal with. When $z_c \to \infty$ the normalization constants of all the wave-functions are predominately those of plane waves, as in this limit

– 10 –
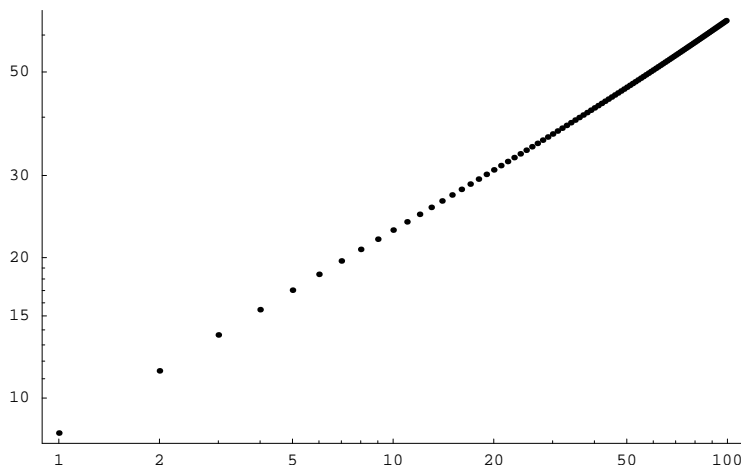
Figure 7: Log~Log plot of the resonance mass M versus k_-k_+ (both axes are scaled by 100).

the solutions we found approach free plane waves. In this case it is easy to calculate the mixing f_m which is given by

$$
\begin{aligned}
f_m &= \epsilon_{1+}\epsilon_{2+}\cos\left(\arctan\alpha_{1+} - \arctan\alpha_{2+}\right) \\
&\quad + \epsilon_{1-}\epsilon_{2-}\cos\left(\arctan\alpha_{1-} - \arctan\alpha_{2-}\right) \\
&= \frac{\epsilon_{1+}\epsilon_{2+}(1 + \alpha_{1+}\alpha_{2+})}{\sqrt{(1 + \alpha_{1+}^2)(1 + \alpha_{2+}^2)}} + \frac{\epsilon_{1-}\epsilon_{2-}(1 + \alpha_{1-}\alpha_{2-})}{\sqrt{(1 + \alpha_{1-}^2)(1 + \alpha_{2-}^2)}}.
\end{aligned}
\tag{3.20}
$$

Here $\epsilon_{1,2\pm}$ are the sign factors for each wave-function as described before and $\alpha_{1,2\pm}$ are the two solutions of equations (2.10) and (2.11). We computed the expression for the mixing coefficients numerically. For any values of the ratio η and mass m, f_m's vanish with an extremely high accuracy (10^{-13} or so). This suggests that the two spectra are indeed orthogonal to each other.

The next question of interest is the mass of the resonance mode, defined as the location of its peak. Unfortunately no analytic solution is known for the dependence of this mass M on k_- and k_+. From symmetry and dimensional analysis, it is reasonable to expect that $M \sim \sqrt{k_-k_+}$. This can be verified numerically as follows. We solve for the mass M numerically for different values of $k_\pm$. A log~log-plot of M versus k_+k_- is shown in figure 7. It suggests that $M \sim \sqrt{k_+k_-}$. We point out that the width of the resonance is always of order of the greatest curvature (k_+).

Finally we would like to comment a bit more on the relation between the asymmetric model and the DGP model. As we have seen, when $k_+ \sim k_-$ the asymmetric and RS models are almost identical and have nothing similar to DGP. When $\eta \ll 1$, we have the following three regions in terms of the distance r as measured on the brane. (1). $r > 1/k_\pm$: Both the asymmetric and RS model approach the same 4-D effective theory, in this regime the zero-mode dominates. (2). $1/k_+ \lesssim r \lesssim 1/k_-$: In this region we can integrate out the bulk space on the k_+ side and this procedure leaves us with an induced 4-D Einstein-Hilbert term in the effective action [10]. Therefore we expect that the theory behaves as

the DGP model with only a half of the bulk space. In the extreme case when the bulk space on one side is flat, we are in this region whenever $r \gtrsim 1/k$, k is the curvature of the AdS side (it should be reminded that no zero mode is present in this extreme case, therefore the previously discussed case does not apply). This is perfectly consistent with what we discussed in section 3.2, where we have shown that the spectrum agrees with that of the DGP model exactly for $r \gg 1/k$. Notice, however, that this region coincides with the domain $r \gg r_c$ in the corresponding DGP model where gravity already switches to the 5-D behavior. (3). $r < 1/k_\pm$: In this region the theory should give rise to 5-D gravitational interactions.

4. Gravitational potential on the brane

It is instructive to compare the asymmetric model with AdS curvatures k_+ and k_- with the RS model in which the curvature k satisfies

$$\frac{1}{2}\left(\frac{1}{k_+} + \frac{1}{k_-}\right) = \frac{1}{k}. \tag{4.1}$$

As long as the above relation holds, the effective Planck mass $M_{\rm pl}$ measured on the brane for both models is the same.

Let us first look at the 2-particles gravitational potentials on the brane-world. They are given by

$$V_{RS}(r) = \frac{1}{M_{pl}^2}\frac{m_1 m_2}{r} + \frac{1}{M_*^3}\int_0^\infty \mathrm{d}m \frac{m_1 m_2 e^{-mr}}{r}\psi_{RS}(0)^{(m)\,2}, \tag{4.2}$$

in the RS, and

$$V_{\rm asym}(r) = \frac{1}{M_{\rm pl}^2}\frac{m_1 m_2}{r} + \frac{1}{M_*^3}\int_0^\infty \mathrm{d}m \frac{m_1 m_2 e^{-mr}}{r}[\psi_1(0)^{(m)\,2} + \psi_2(0)^{(m)\,2}], \tag{4.3}$$

in the asymmetric model. It is hard to calculate the integrals analytically but numerical comparison between the two model can be done. Figure 8 shows the ratio $V_{\rm asym}/V_{RS}$ versus $\eta = k_-/k_+$. Each curve represents $V_{\rm asym}/V_{RS}$ measured at a fixed r. For dashed curves, from bottom to up, $r\,k_+ = 25, 5, 1$ respectively, and for solid curves, from top to down, $r\,k_+ = 1/5, 1/10, 1/50$. As expected, when $\eta \to 1$, the two potentials are equal at all distances. While for $\eta \neq 1$ they are mostly different at distances comparable to $1/\sqrt{k_+ k_-} \sim 1/M_{\rm res}$.

A plot of $V_{\rm asym}/V_{RS}$ versus $r\,k_+$ with a fixed value of $\eta = 0.2$ is presented on figure 8. At very short distances, both models approach the usual 5-D theory. At very large distances, the zero-mode in both models dominates and gives rise to the same 4-D gravitational potentials (we should stress that we have fixed the effective 4-D Planck mass to be the same for both models). The largest departure is at scales comparable to $1/M_{\rm res}$, where the resonance is not exponentially suppressed in the integral in (4.3).
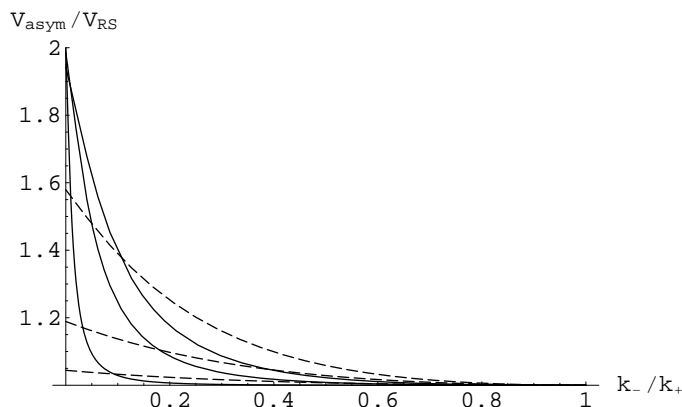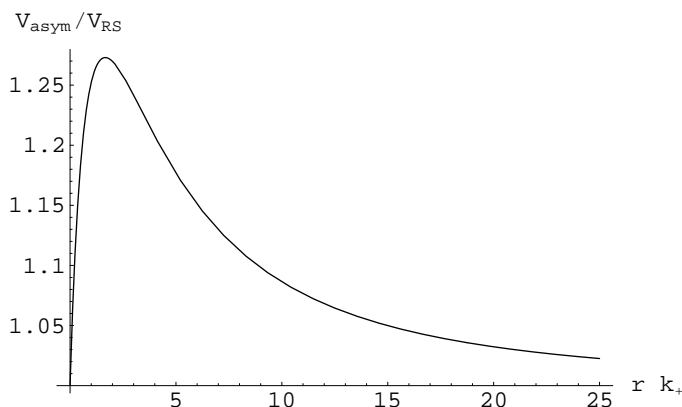
Figure 8: $V_{\text{asym}}(r)/V_{RS}(r)$ versus η.

Figure 9: $V_{\text{asym}}(r)/V_{RS}(r)$ versus $r\,k_+$.

5. Comments on holographic correspondence

The AdS/CFT (holographic) correspondence [11 – 13] provides a powerful tool to explore strongly coupled field theories by looking at their weakly coupled gravity duals. The holographic correspondence for the RS2 model has been studied in great detail. AdS gravity is dual to a conformal field theory (CFT) in lower dimension, and the presence of the brane in the RS2 model gives rise to a UV cut-off and to a massless 4D graviton on the CFT side. The main evidence for the duality between RS and a UV cut-off CFT coupled to 4D gravity were obtained in refs. [14 – 16]: The leading correction to the braneworld Newton potential found by RS on the gravity side is reproduced by one-loop correction to the graviton propagator in CFT [14, 15]. This radiative correction is evaluated from the one-loop graviton self-energy graph where only the CFT fields are running in the loop. For any 4D massless theory the finite part of such a loop is proportional to $\log(p_E^2)$, where p_E^2 is an euclidean momentum square flowing through the loop diagram. This term, after

Fourier transformation, gives the $1/r^3$ correction to the Newton potential which exactly matches the correction due to the bulk KK gravitons [15]. Furthermore, the very same calculation suggests the following dictionary: the RS2 model with bulk curvature k^2 is dual to SU(N) CFT with $N^2 \sim M_\star^3/k^3$, where $M_\star$ is the Planck mass of 5D gravity. The field theory UV cut-off Λ is proportional to the curvature scale k.

It is reasonable to expect that the holographic dual also exists for the asymmetric braneworld. Schematically, the dual of the asymmetric warped braneworld would be a theory that consists of two sectors, $CFT_- \otimes CFT_+$, with number of colors $N_\pm^2 \sim M_\star^3/k_\pm^3$ and cut-off scales $\Lambda_\pm \sim k_\pm$ respectively. It is expected that the resonance is dual to a composite state of $CFT_+ \otimes CFT_-$, made of states living in both CFT's. Its presence is due to the interaction terms, which have to be proportional to the difference of the two curvatures, so that in the limit $\eta \to 1$ the composite state disappears from the spectrum.

Assuming for definiteness that $\Lambda_+ > \Lambda_-$, we can integrate out the modes with energies between Λ_- and Λ_+ in the CFT_+ sector. The resulting low-energy effective field theory reduces to $CFT_+ \otimes CFT_-$ with the common UV cutoff Λ_-, an additional induced cosmological constant (which has to be tuned to zero) and, most importantly, the induced EH term. The coefficient of the latter is proportional to the difference between Λ_+ and Λ_-, and can be evaluated by "integrating out" [16], [17] a slab of the AdS space between $1/k_+$ and $1/k_-$

$$2M_\star^3 \int_{1/k_+}^{1/k_-} \mathrm{d}z \frac{1}{k_+^3 z^3} \int \mathrm{d}^4 x \sqrt{-g^{(4)}} R^{(4)} = M_\star^3 \frac{k_+^2 - k_-^2}{k_+^3} \int \mathrm{d}^4 x \sqrt{-g^{(4)}} R^{(4)}. \qquad (5.1)$$

Except for this term, the resulting effective theory resembles the RS2 model. On the other hand, RS2 is dual to CFT, not to $CFT \otimes CFT$. This difference is due to the orbifold projection imposed in RS, which results in the removal of the antisymmetric gravitational perturbation from the spectrum. In the effective low energy theory of the asymmetric braneworld, no such a projection is imposed, and, therefore, both symmetric and antisymmetric modes are retained. Hence, the product structure $CFT_+ \otimes CFT_- \to CFT_{\text{sym}} \otimes CFT_{\text{asym}}$ emerges. However, in the low-energy regime, only symmetric modes are coupled to the brane localized 4D matter, while the antisymmetric ones are null on the brane. Because of this, one of the two CFT's in the low energy theory will not couple directly to the 4D matter. The effects of the high-scale coupling of this CFT to the localized matter are encoded, in the low energy theory, in the induced EH term. This is consistent with the earlier observation that the resonance is above the cutoff Λ_-.

6. Conclusions

We have studied in detail the spectrum of gravitational perturbations in a brane-world scenario with asymmetric warped geometry. We have shown that even when the two AdS curvatures $k_\pm^2$ are different, the RS zero-mode still exists. Its strength on the brane is given by $\sim [2k_+ k_-/(k_+ + k_-)]^{1/2}$, which vanishes if one side of the brane becomes space-time flat.

A novelty is found in the massive KK graviton spectrum.[5] When the warp factors are different, there exists a resonance mode in addition to the RS-like spectrum. The peak of this resonance is located at $M \sim \sqrt{k_+ k_-}$ and it has a width of the order of the larger curvature scale. As the asymmetry between $k_+ \neq k_-$ grows, the zero-mode becomes weaker and partially transmutes into the resonance mode. In the limit when the bulk space-time on one side of the brane is flat, the resonance mode reaches its maximal strength while the zero-mode is no longer normalizable and disappears from the spectrum. On the gravity side we studied numerically the 2-body gravitational potential measured on the brane-world, and discussed the holographic description of the asymmetric model. The obtained results can be useful for the particle physics model building via the AdS/CFT correspondence, as well as for the cosmology of early universe when studied in the context of warped space-times.

Acknowledgments

References

[1] L. Randall and R. Sundrum, *An alternative to compactification*, *Phys. Rev. Lett.* **83** (1999) 4690 [hep-th/9906064].

[2] M. Cvetič, S. Griffies and S.-J. Rey, *Static domain walls in $N = 1$ supergravity*, *Nucl. Phys.* **B 381** (1992) 301 [hep-th/9201007];
M. Cvetič, S. Griffies and S.-J. Rey, *Nonperturbative stability of supergravity and superstring vacua*, *Nucl. Phys.* **B 389** (1993) 3 [hep-th/9206004].

[3] A. Padilla, *Infra-red modification of gravity from asymmetric branes*, *Class. and Quant. Grav.* **22** (2005) 1087 [hep-th/0410033]; *Cosmic acceleration from asymmetric branes*, *Class. and Quant. Grav.* **22** (2005) 681 [hep-th/0406157].

[4] K. Koyama and K. Koyama, *Brane induced gravity from asymmetric compactification*, *Phys. Rev.* **D 72** (2005) 043511 [hep-th/0501232].

[5] O. Castillo-Felisola, A. Melfo, N. Pantoja and A. Ramirez, *Localizing gravity on exotic thick 3-branes*, *Phys. Rev.* **D 70** (2004) 104029 [hep-th/0404083];
R. Guerrero, A. Melfo, N. Pantoja and R.O. Rodriguez, *Close to the edge: hierarchy in a double braneworld*, hep-th/0605160.

[6] G.R. Dvali, G. Gabadadze and M. Porrati, *Metastable gravitons and infinite volume extra dimensions*, *Phys. Lett.* **B 484** (2000) 112 [hep-th/0002190].

---

[5]In ref. [18] quasi-normal states were argued to exist in the standard RS spectrum (we thank Roy Maartens for bringing this reference to our attention). It would be interesting to see if similar states also appear in the asymmetric part of the spectrum discussed in the present work.

[7] E. Kiritsis, N. Tetradis and T.N. Tomaras, *Induced gravity on RS branes*, *JHEP* **03** (2002) 019 [`hep-th/0202037`].

[8] R. Gregory, V.A. Rubakov and S.M. Sibiryakov, *Opening up extra dimensions at ultra-large scales*, *Phys. Rev. Lett.* **84** (2000) 5928 [`hep-th/0002072`];
C. Csáki, J. Erlich and T.J. Hollowood, *Quasi-localization of gravity by resonant modes*, *Phys. Rev. Lett.* **84** (2000) 5932 [`hep-th/0002161`];
G.R. Dvali, G. Gabadadze and M. Porrati, *Metastable gravitons and infinite volume extra dimensions*, *Phys. Lett.* **B 484** (2000) 112 [`hep-th/0002190`].

[9] L. Randall and R. Sundrum, *A large mass hierarchy from a small extra dimension*, *Phys. Rev. Lett.* **83** (1999) 3370 [`hep-ph/9905221`].

[10] G.R. Dvali, G. Gabadadze, M. Kolanovic and F. Nitti, *Scales of gravity*, *Phys. Rev.* **D 65** (2002) 024031 [`hep-th/0106058`].

[11] J.M. Maldacena, *The large-N limit of superconformal field theories and supergravity*, *Adv. Theor. Math. Phys.* **2** (1998) 231 [`hep-th/9711200`].

[12] E. Witten, *Anti-de Sitter space and holography*, *Adv. Theor. Math. Phys.* **2** (1998) 253 [`hep-th/9802150`].

[13] S.S. Gubser, I.R. Klebanov and A.M. Polyakov, *Gauge theory correlators from non-critical string theory*, *Phys. Lett.* **B 428** (1998) 105 [`hep-th/9802109`].

[14] S.S. Gubser, *AdS/CFT and gravity*, *Phys. Rev.* **D 63** (2001) 084017 [`hep-th/9912001`].

[15] M.J. Duff and J.T. Liu, *Complementarity of the Maldacena and Randall-Sundrum pictures*, *Phys. Rev. Lett.* **85** (2000) 2052 [`hep-th/0003237`].

[16] N. Arkani-Hamed, M. Porrati and L. Randall, *Holography and phenomenology*, *JHEP* **08** (2001) 017 [`hep-th/0012148`].

[17] M. Redi, *Brane running and AdS/CFT*, *JHEP* **05** (2003) 032 [`hep-th/0304014`].

[18] S.S. Seahra, *Ringing the Randall-Sundrum braneworld*, *Phys. Rev.* **D 72** (2005) 066002 [`hep-th/0501175`].